Self-Noise Models of Five Commercial Strong-Motion Accelerometers

by A. T. Ringler, J. R. Evans, and C. R. Hutt

INTRODUCTION

Strong-motion accelerometers provide onscale seismic recordings during moderate-to-large ground motions (e.g., up to tens of m/s^2 peak). Such instruments have played a fundamental role in improving our understanding of earthquake source physics (Bock *et al.*, 2011), earthquake engineering (Youd *et al.*, 2004), and regional seismology (Zollo *et al.*, 2010). Although strong-motion accelerometers tend to have higher noise levels than high-quality broadband velocity seismometers, their higher clip-levels provide linear recordings at near-field sites even for the largest of events where a collocated broadband sensor would no longer be able to provide onscale recordings (Clinton and Heaton, 2002).

Recently, the seismological community has begun to make use of strong-motion accelerometer data even in the absence of large ground motions (e.g., Tibuleac *et al.*, 2011). The noise floor of the instruments often limits the usefulness of strong-motion accelerometer data in such studies, because it obscures first arrivals or can make the traces dominated by noise. When a strong-motion accelerometer is deployed in a quiet setting, the noise floors of the digitizer and the accelerometer tend to dominate the other noise sources (Cauzzi and Clinton, 2013). This situation is unlike that using broadband sensors, in which site conditions are typically the largest contributing source of noise in seismic data, especially at long periods (Wilson *et al.*, 2002). With the widespread deployment of strong-motion accelerometers recorded on high resolution digitizers, it is now possible to get continuous high-rate acceleration data in which the digitizer noise is not the dominant noise source (Cauzzi and Clinton, 2013).

To better characterize the noise of a number of commonly deployed accelerometers in a standardized way, we conducted noise measurements on five different models of strong-motion accelerometers. Our study was limited to traditional accelerometers (Fig. 1) and is in no way exhaustive. We have not looked at any microelectromechanical system sensors or other low-cost sensors (e.g., Evans *et al.*, 2014). Our approach is similar to the tests we previously conducted on broadband sensors (Ringler and Hutt, 2011). However, the elevated self-noise of strong-motion accelerometers in conjunction with the low site noise in the Albuquerque Seismological Laboratory's (ASL) underground vault (Fig. 2) allows us to get accurate estimates of strong-motion accelerometer self-noise without using coherence analysis techniques (e.g., Holcomb, 1989, or Sleeman *et al.*, 2006; Evans *et al.*, 2010; Ringler *et al.*, 2011). Of course, this is only true when the accelerometer's self-noise is well above the site noise (Fig. 2) and the digitizer noise. This approach also helps to minimize the accelerometers sensitivity to nonseismic noise sources that can contribute to the noise for shallow vault installations (Cauzzi and Clinton, 2013) and avoids additional complications where data rotation is required (Gerner and Bokelmann, 2013).

We hope that our noise tests will help to better characterize current sensor performance and to provide a useful reference for understanding the self-noise of a number of off-the-shelf strong-motion accelerometers. These self-noise levels can be used as a reference for noise-testing instruments prior to the instruments being deployed.

METHODS

Each sensor was installed in the ASL underground vault (~10 m of overburden) in which the instruments were thermally isolated and background noise was recorded on Quanterra Q330 or Quanterra Q330HR digitizers (Quanterra, 2007) at 200 samples/s. In order to avoid digitizer noise, we recorded with a pre-amplifier gain of ×20 or ×30 (Fig. 2). For each model of sensor, we tested five units, and for each unit, we picked quiet time segments (each time segment included data from the vertical and two horizontal components). By limiting our tests to a small number of time segments, noise variations over time could be hidden (Sleeman and Melichar, 2012). The 15 time segments (three components on five sensors) being used were each 3500 s long. The accelerometers' noise levels are above that of the site noise with the possible exception of the 4–8 s microseism period band. We did not make any distinction between horizontal or vertical components because the instrument noise in accelerometers is well above the typical tilt noise that dominates horizontal broadband sensors (Zürn *et al.*, 2007). Using these time series, we then estimated power spectra for each of the sensors under test, with the Welch averaging method (Welch, 1967). We used time windows of 2^{14} samples with 7/8th overlap with the linear trend removed and a Hamming taper applied. The lack of a large visual microseismic peak in the power spectra further confirms that the site noise was well below the instrument self-noise at frequencies greater than 0.25 Hz (Fig. 3).

RESULTS

The self-noise estimates for each of the six tested instruments (five different models) are shown in Figure 3. We included

doi: 10.1785/0220150027

▲ **Figure 1.** Examples of the strong-motion accelerometers used in this test. The Kinemetrics EpiSensor ES-T has the same case as the Kinemetrics EpiSensor ES-T Nickel (not shown). Each tile is approximately 0.3 m.

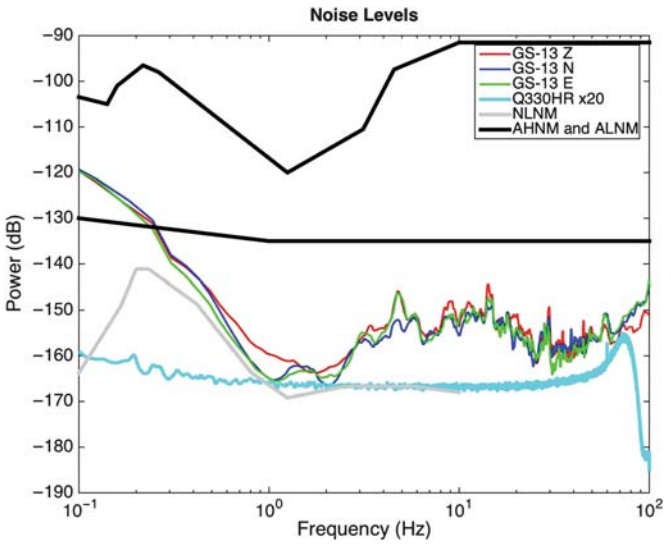

▲ **Figure 2.** Typical high-frequency vault noise in the Albuquerque Seismological Laboratory (ASL) vault, recorded on a GS-13 for the vertical (red), north–south (blue), and east–west (green) when the AC power is turned off in the vault. The Peterson new low-noise model (NLNM; Peterson, 1993) is shown in gray, and the accelerometer high- and low-noise models (AHNM and ALNM; Cauzzi and Clinton, 2013) are shown in black. We also included the self-noise of a Quanterra Q330HR with a ×20 pre-amp corrected for an accelerometer sensitivity of 10 V/*g*.

noise estimates for the modified Kinemetrics EpiSensor and the nickel-plated version but are considering them the same model of sensor. For each instrument under evaluation, five different sensors were tested concurrently. For each of the subplots in Figure 3, we included the Peterson new low-noise model (NLNM; Peterson, 1993) for reference. We removed the sensitivity and response of the instrument (Fig. 4) as well as the sensitivity of the digitizer and amplifier, so all results are shown in decibels (dB) relative to $1(m/s^2)^2/Hz$. The sensitivity of many of the accelerometers tested can be changed as desired by the user. In these cases, we just listed the sensitivity used during our tests (Table 1). In theory, increasing the sensitivity by a factor of two should decrease the noise level of the sensor by 6 dB. However, additional complications arise because increasing the gain does not improve the noise of the electronic and mechanical components, which eventually becomes a fundamental limiter.

We note that the elevated noise levels of some of the GeoTech PA-23 power spectra in the 10–40 Hz frequency band are not isolated to a single sensor (Fig. 3a). We are unable to explain the decrease in instrument noise at 30 Hz of the Güralp CMG-5TC (Fig. 3b); however, because the lowered noise levels are near the corner frequency of the instrument it could be that the response needs to be described using a more complicated response model, which we did not pursue. The Kinemetrics EpiSensor ES-T (Fig. 3c) noise measurements showed one sensor channel had elevated noise and there was relatively more scatter at higher frequencies (e.g., 10 Hz and greater) than the Nickel version. The Kinemetrics EpiSensor ES-T Nickel (Fig. 3d) sensors are similar to the original EpiSensor ES-T (Fig. 3c), but the zinc plating on some of the components was replaced with nickel plating. We have included both for completeness. The nickel-plated version of the EpiSensor ES-T shows less variability in noise levels between components as compared to the version without nickel plating. The Nanometrics Titan accelerometers (Fig. 3e) all had similarly low noise levels across the entire frequency band. One of the channels of the REF TEK 147-01/3 (Fig. 3f) showed elevated noise and was included in the results for consistency. Because the median is a robust estimator and we were not able to conduct the tests again, we did not remove this trace. However, this did not substantially change the low and median self-noise models discussed below.

Summary Results

Using the results from Figure 3, we were able to estimate low and median self-noise models for all of the sensors (Figs. 5 and 6). These estimates were taken pointwise, so potentially no single instrument has a self-noise as low as the low noise estimated. However, such estimates do give an indication of what the typical (median) and low self-noise of one of the instruments tested might be in an ideal situation. For reference, we included the results with Cauzzi and Clinton (2013) in both Figures 4 and 5. From Figure 4, we see that the Cauzzi and Clinton accelerometer low-noise model (ALNM) could potentially be defined by the self-noise of the instruments used in the study and not necessarily the site conditions or installation methods at frequencies from 0.1 to 10 Hz. At frequencies greater than 1 Hz, Cauzzi and Clinton define their ALNM to be a constant −135 dB, which results in a lower noise estimate than we are able to resolve with our measured self-noise

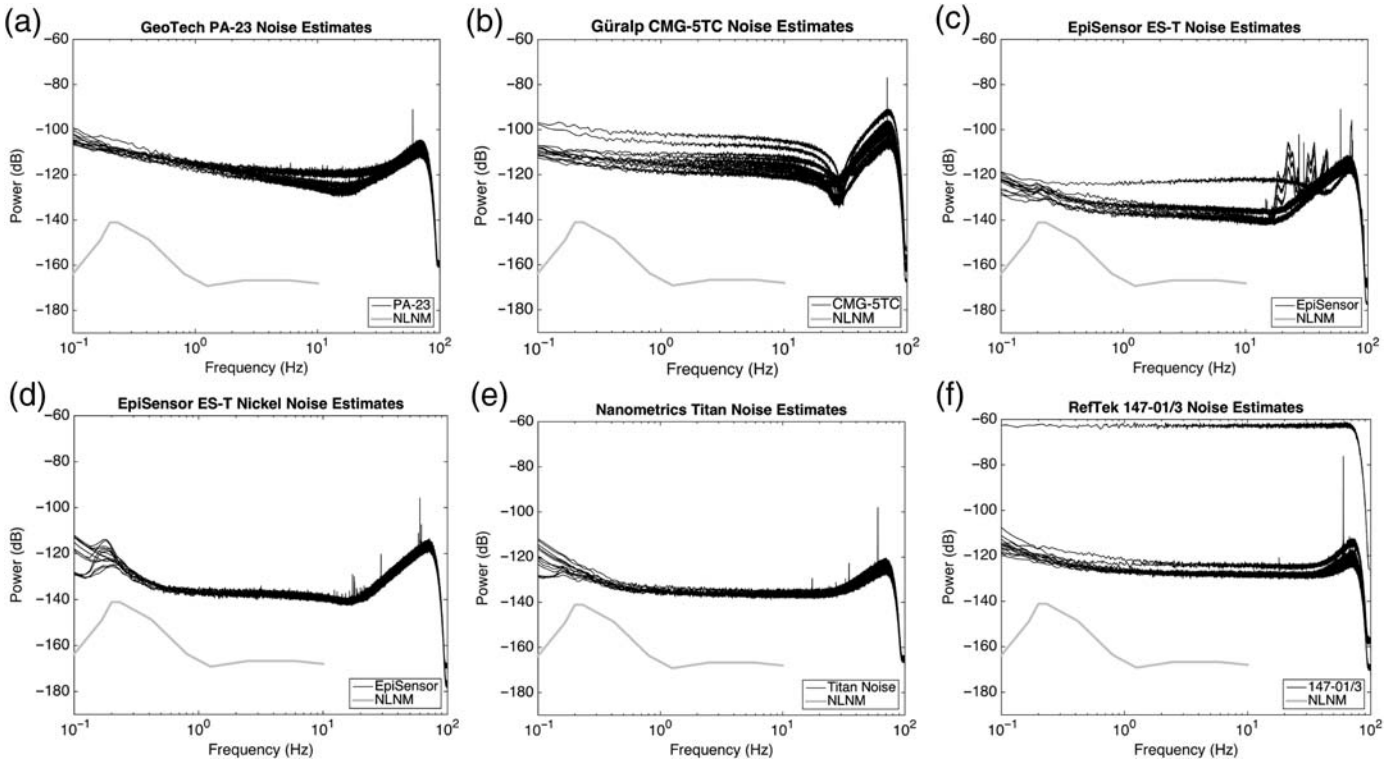

▲ **Figure 3.** Self-noise estimates from 15 different time series for each of the different models of strong-motion accelerometers used in this study: (a) GeoTech PA-23, (b) Güralp CMG-5TC, (c) Kinemetrics EpiSensor ES-T, (d) Kinemetrics EpiSensor ES-T Nickel, (e) Nanometrics Titan, and (f) REF TEK 147-01/3. We included the Peterson NLNM (Peterson, 1993) for reference (thick gray line).

estimates. We limited ourselves to using robust estimators to avoid skewing our self-noise estimates when there were a couple of channels with potentially elevated self-noise.

As can be seen, all accelerometers show elevated self-noise beyond the frequency corner of the instrument (Fig. 3). This is likely caused by the lowered gain at these higher frequencies in the feedback loop (Wielandt, 2002). Because most feedback accelerometers use a displacement sensor to measure the motion of the proof mass, the self-noise of the instrument will rise like the self-noise of the displacement sensor multiplied by the inverse of the spring mass systems' acceleration response to a constant displacement, which is the square of the frequency (Ian Standley, personal comm., 2015). At frequencies near 100 Hz, we see that all spectra roll off, which is caused by the finite impulse response filters in the digitizer.

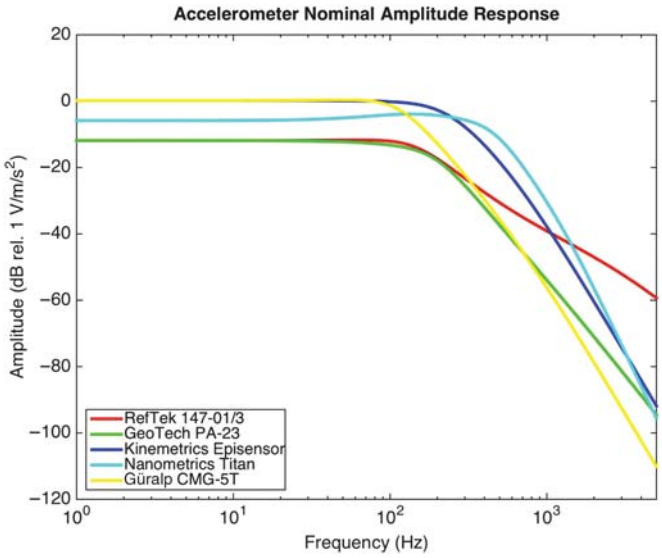

▲ **Figure 4.** Nominal amplitude responses for the strong-motion accelerometers used in this article. The Kinemetrics EpiSensor ES-T and EpiSensor ES-T Nickel have identical responses.

CONCLUSIONS

We estimated the self-noise of five different commercial strong-motion accelerometers commonly used in seismic studies. Our tests were all conducted in a quiet vault where the site noise was below that of the instrument noise, allowing us to avoid using coherence methods while still getting reliable estimates of the self-noise of the instruments because there are no coherent ground-motion singles to remove when the vault noise is well below the instrument self-noise (Ringler *et al.*, 2011).

Our ability to detect small seismic signals is fundamentally limited by the self-noise of an instrument in conjunction with datalogger self noise and the site noise. At many seismic stations where the vaults are temperature stable, the self-noise of an accelerometer could be above the site noise, making sensor noise one of the fundamental limitations in detecting small

Table 1
Sensor Model Used in the Test, Associated Vendor, Sensitivity of Accelerometer, Full-Scale Output, and Associated Subplot in Figure 3 for the Strong-Motion Accelerometers in Our Study

Sensor	Vendor	Sensitivity (V/*g*)	Full Scale Output (*g*)	Figure
PA-23	GeoTech	2.5	±4	3a
CMG-5TC	Güralp	5	±2	3b
EpiSensor ES-T	Kinemetrics	10	±2	3c
EpiSensor ES-T Nickel	Kinemetrics	10	±2	3d
Titan	Nanometrics	5	±4	3e
147-01/3	REF TEK	2.5	±4	3f

The corresponding response models are shown in Figure 4.

seismic signals. From Figure 6, we see that even in the best cases the ALNM is only a few decibels above the self-noise of the lowest noise instruments from 0.1 to 10 Hz. This suggests that there are fielded accelerometers where the self-noise of the instrument is limiting our ability to detect small seismic signals. This leads us to the need for higher dynamic range accelerometers, accelerometers with lower noise floors, or accelerometers collocated with a lower noise broadband seismometer to ensure onscale recordings of both small and large ground motions.

Although instrument noise is one of the fundamental limitations in strong-motion seismology, other instrument specifications also need to be considered when looking at the performance of any seismic instrument (Hutt *et al.*, 2009). As with any seismic instrument, other key factors such as the instrument's sensitivity to nonseismic sources, cost, and reliability also play a role. Variable noise among channels of the same sensor type, dead channels, or other anomalous elevated noise on accelerometers should be examined by the manufacturer. Using the self-noise models produced in this article, or similar types of self-noise models, it is possible to test a particular instrument and verify that it has sufficiently low noise for its intended application. Such comparisons could also warn a user of a potentially problematic sensor component (e.g., Fig. 3f). Thus, when selecting an instrument to install at a particular site, other tests and specifications should also be considered. Sensor self-noise should not be the sole consideration. When selecting an instrument, characteristics like reliability, total dynamic range, and other measureable specifications should also be considered. Some of these additional specifications, which are beyond the scope of this article, are described in Hutt *et al.* (2009).

ACKNOWLEDGMENTS

The authors thank GeoTech, Güralp, Kinemetrics, Nanometrics, and REF TEK for useful discussions and help with verifying the appropriate tests setups. We thank an anonymous

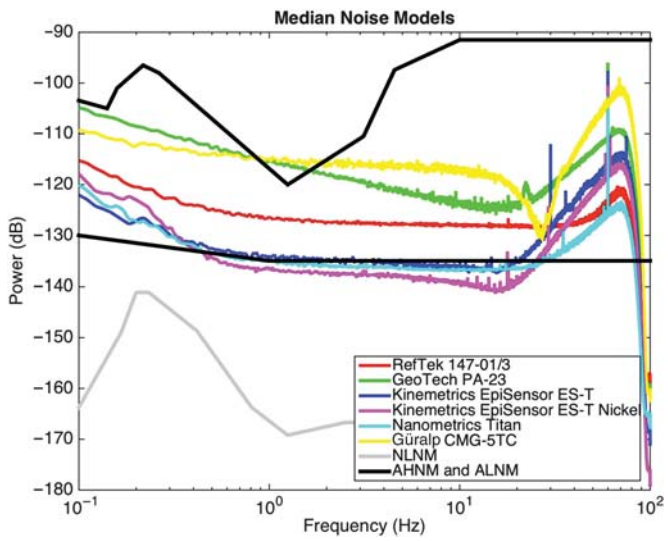

▲ **Figure 5.** Pointwise median self-noise estimates from 15 different power spectra for each sensor. The Peterson NLNM (Peterson, 1993) is shown in gray, and the AHNM and ALNM (Cauzzi and Clinton, 2013) are shown in black.

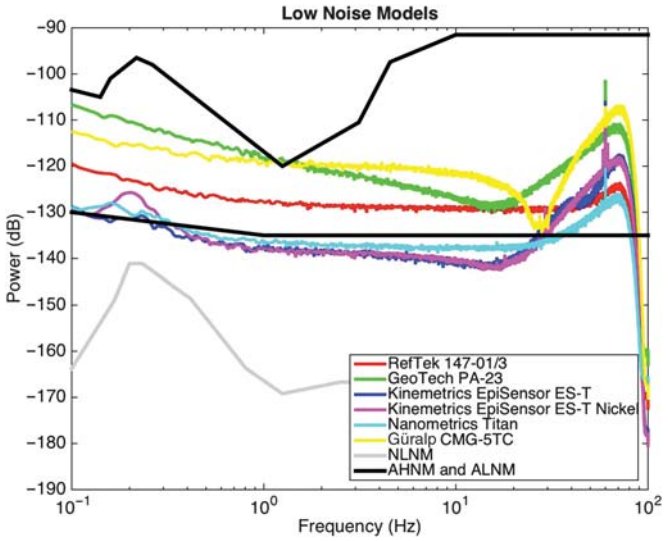

▲ **Figure 6.** Pointwise minimum low self-noise estimates from 15 different power spectra from each model. The Peterson NLNM (Peterson, 1993) is shown in gray, and the AHNM and ALNM (Cauzzi and Clinton, 2013) are shown in black.

reviewer, Carlo Cauzzi, John Clinton, Jill McCarthy, Zhigang Peng, Janet Slate, and Danielle Sumy for their helpful reviews of the article. We thank L. S. Gee and D. Wilson for other useful discussions pertaining to instrument self-noise. Finally, we thank Tom de la Torre for help in conducting the self-noise tests.

Any use of trade, product, or firm names is for descriptive purposes only and does not imply endorsement by the U.S. Government.

REFERENCES

Bock, Y., D. Melgar, and B. W. Crowell (2011). Real-time strong-motion broadband displacements from collocated GPS and accelerometers, *Bull. Seismol. Soc. Am.* **101,** 2904–2925, doi: 10.1785/0120110007.

Cauzzi, C., and J. Clinton (2013). A high- and low-noise model for high-quality strong-motion accelerometer stations, *Earthq. Spectra* **29,** 85–201, doi: 10.1193/1.4000107.

Clinton, J. F., and T. H. Heaton (2002). Potential advantages of a strong-motion velocity meter over a strong-motion accelerometer, *Seismol. Res. Lett.* **73,** 332–342, doi: 10.1785/gssrl.73.3.332.

Evans, J. R., R. M. Allen, A. I. Chung, E. S. Cochran, R. Guy, M. Hellweg, and J. F. Lawrence (2014). Performance of several low-cost accelerometers, *Seismol. Res. Lett.* **85,** 147–159, doi: 10.1785/0220130091.

Evans, J. R., F. Followill, C. R. Hutt, R. P. Kromer, J. M. Steim, R. L. Nigbor, A. T. Ringler, and E. Wielandt (2010). Method for calculating self-noise spectra and operating ranges for seismographic inertial sensors and recorders, *Seismol. Res. Lett.* **81,** 640–646, doi: 10.1785/gssrl.81.4.640.

Gerner, A., and G. Bokelmann (2013). Instrument self-noise and sensor misalignment, *Adv. Geosci.* **36,** 17–20, doi: 10.5194/adgeo-36-17-2013.

Holcomb, L. G. (1989). A direct method for calculating instrument noise levels in side-by-side seismometer evaluations, *U.S. Geol. Surv. Open-File Rept. 89-214,* 34 pp.

Hutt, C. R., J. R. Evans, F. Followill, R. L. Nigbor, and E. Wielandt (2009). Guidelines for standardized testing of broadband seismometers and accelerometers, *U.S. Geol. Surv. Open-File Rept. 2009-1295,* 62 pp.

Peterson, J. (1993). Observations and modeling of seismic background noise, *U.S. Geol. Surv. Open-File Rept. 93-322,* 94 pp.

Quanterra (2007). *Q330 Operation Guide: Q330HR/Q330 Operation Overview of Support Tools Baler Operation*, Document Number 304808, 318 pp.

Ringler, A. T., and C. R. Hutt (2011). Self-noise models of seismic instruments, *Seismol. Res. Lett.* **81,** 972–983, doi: 10.1785/gssrl.81.6.972.

Ringler, A. T., C. R. Hutt, J. R. Evans, and L. D. Sandoval (2011). A comparison of seismic instrument self-noise analysis techniques, *Bull. Seismol. Soc. Am.* **101,** 558–567, doi: 10.1785/0120100182.

Sleeman, R., and P. Melichar (2012). A PDF representation of the STS-2 self-noise obtained from one year of data recorded in the Conrad Observatory, Austria, *Bull. Seismol. Soc. Am.* **102,** 587–597, doi: 10.1785/0120110150.

Sleeman, R., A. van Wettum, and J. Trampert (2006). Three-channel correlation analysis: A new technique to measure instrument noise of digitizers and seismic sensors, *Bull. Seismol. Soc. Am.* **96,** 258–271, doi: 10.1785/0120050032.

Tibuleac, I. M., D. H. von Seggern, J. G. Anderson, and J. N. Louie (2011). Computing Green's functions from ambient noise recorded by accelerometers and analog, broadband, and narrow-band seismometers, *Seismol. Res. Lett.* **82,** 661–675, doi: 10.1785/gssrl.82.5.661.

Welch, P. D. (1967). The use of fast Fourier transform for the estimation of power spectra: A method based on time averaging over short, modified periodograms, *IEEE Trans. Audio* **AU-15,** 70–73, doi: 10.1109/TAU.1967.1161901.

Wielandt, E. (2002). Seismic sensors and their calibration, in *New Manual of Seismological Observatory Practices*, 1-467, GeoForschungsZentrum Potsdam, http://bib.telegrafenberg.de/publizieren/vertrieb/nmsop/ (last accessed May 2015).

Wilson, D., J. Leon, R. Aster, J. Ni, J. Schue, S. Grand, S. Semken, S. Baldridge, and W. Gao (2002). Broadband seismic background noise at temporary seismic stations observed on a regional scale in the southwestern United States, *Bull. Seismol. Soc. Am.* **92,** 3335–3341, doi: 10.1785/0120010234.

Youd, T., J. Steidl, and R. Nigbor (2004). Lessons learned and the need for instrumented liquefaction sites, *Soil Dyn. Earthq. Eng.* **24,** 9–10, doi: 10.1016/j.soildyn.2004.06.006.

Zollo, A., O. Amoroso, M. Lancieri, Y. M. Wu, and H. Kanamori (2010). A threshold-based earthquake early warning using dense accelerometer networks, *Geophys. J. Int.* **183,** 963–974, doi: 10.1111/j.1365-246X.2010.04765.x.

Zürn, W., J. Exß, H. Steffen, C. Kroner, T. Jahr, and M. Westerhaus (2007). On reduction of long-period horizontal seismic noise using local barometric pressure, *Geophys. J. Int.* **171,** 780–796, doi: 10.1111/j.1365-246X.2007.03553.x.

A. T. Ringler
C. R. Hutt
U.S. Geological Survey
Albuquerque Seismological Laboratory
P.O. Box 82010
Albuquerque, New Mexico 87198 U.S.A.
aringler@usgs.gov

J. R. Evans
U.S. Geological Survey
400 Natural Bridges Drive
Santa Cruz, California 95060 U.S.A.

Published Online 20 May 2015